A Variational Semi-Analytical Approach for Efficient Analysis of Multilayer Discrete-Jacketed Cylindrical Vessels

Yubo Huang[1], Bao Wang[1*], Jiahui Liang[1], Lei Zhang[2]

[1]CISRI HIPEX Technology Co., Ltd, China Iron & Steel Research Institute Group
[2]Department of Mechanical Engineering, Tsinghua University

*Corresponding author, email: wangbao@hipex.cn

Abstract

Discrete jacket structures have been increasingly applied in high-pressure vessels to achieve thermal–mechanical decoupling under extreme operating conditions. In this study, a multilayer discrete-jacketed configuration is proposed for warm isostatic pressing (WIP) systems, where the discrete jackets are introduced to provide independent thermal management and structural load-bearing functions. However, the complex mechanical response introduced by discrete jacket configurations remains difficult to effectively characterize through conventional analytical formulations. This study proposes a variational energy-based semi-analytical framework for the efficient analysis of multilayer wire-wound cylindrical vessels with discrete jackets. By treating the discrete jacket regions as equivalent cylindrical layers with zero hoop stress, the mechanical response of multilayer structures subjected to internal and external pressures is formulated through an energy minimization approach. A semi-analytical procedure is developed to obtain the stiffness matrix and equivalent load vector from the energy functional, and the framework is further extended to evaluate sequential wire-winding processes through compensated stepwise winding stresses. Finite element simulations demonstrate good agreement between the proposed framework and numerical results in predicting stress distributions. The developed framework provides an efficient tool for the analysis and design of complex multilayer prestressed vessels with discrete jacket configurations.

Key words: Multilayer cylindrical structure with discrete jackets; Variational energy method; Operator identifications; Computational mechanics; Finite element analysis

1. Introduction

High-pressure thermomechanical vessels have been widely employed in various advanced manufacturing and industrial processes where extreme pressure and temperature environments are required. Typical applications include hot extrusion systems, hot isostatic pressing equipment, high-pressure reactors, and other process vessels involving coupled thermal and mechanical loading conditions. In these systems, the pressure-bearing structure is usually subjected to severe stress states due to the combination of high internal pressure, elevated temperature, and complex structural constraints. Therefore, the development of reliable design methodologies for high-pressure thermomechanical vessels has attracted continuous attention in both industrial practice and academic research.

In recent years, the rapid development of solid-state battery technologies has stimulated increasing interest in advanced high-pressure processing techniques for battery manufacturing. Isostatic pressing has been recognized as a promising processing route for solid-state batteries due to its capability of applying uniform compressive stress and improving the densification of solid electrolyte and electrode components. Dixit et al. reviewed the potential role of isostatic pressing in the scalable production of solid-state batteries and highlighted its advantages in improving material consolidation and manufacturing compatibility [1]. Furthermore, experimental studies have demonstrated that isostatic pressing can enhance the compactness of solid electrolyte/electrode composites and improve interfacial contact, thereby reducing internal defects and improving electrochemical performance [2]. Among various isostatic pressing techniques, warm isostatic pressing (WIP) has attracted particular attention because it enables simultaneous application of elevated temperature and quasi-hydrostatic pressure. Recent investigations have demonstrated that WIP treatment can effectively reduce internal voids in composite cathodes and improve the electrochemical properties of all-solid-state lithium-ion batteries, indicating its potential for next-generation battery manufacturing [3]. Consequently, WIP technology has become an important candidate for the post-processing and densification of advanced solid-state battery components.

However, the processing requirements of solid-state battery manufacturing impose unprecedented challenges on the design of WIP equipment. Battery-related WIP applications may require simultaneous exposure to temperatures above 150 °C and ultra-high pressures exceeding 600 MPa. Under such extreme conditions, directly integrating heating elements inside the pressure chamber becomes increasingly difficult due to limitations associated with electrical insulation, sealing reliability, thermal management, and structural integrity. The severe coupling between the heating system and pressure-bearing components may significantly increase design complexity and reduce operational reliability.

Therefore, a decoupled structural configuration, in which the heating and pressurization functions are separated, provides a promising solution for next-generation WIP equipment. In such designs, the pressure vessel is primarily responsible for resisting the ultra-high internal pressure, while the thermal field is generated and controlled through independent heating components. This concept enables more flexible thermal management and improves the long-term reliability of the equipment under extreme operating conditions.

Based on the concept of thermal–mechanical decoupling, discrete jacket structures have been increasingly considered for advanced pressure vessels subjected to severe thermomechanical environments. The fundamental concept is to employ circumferentially distributed discrete structural elements, such as plates or bars, as an external jacket layer surrounding the pressure-bearing cylinder. In this configuration, the vessel wall can be separated into multiple structural regions, while the gaps between adjacent jacket elements provide flow channels for cooling or heating media. Such a configuration enables independent thermal management of the external jacket while maintaining the pressure-bearing function of the inner cylinder. Compared with conventional continuous jacket structures, discrete jacket configurations provide several notable advantages. First, the separation between the thermal management system and the pressure-bearing structure improves the adaptability and reliability of vessels operating under extreme temperature and pressure conditions. Second, unlike integrally fabricated jackets with machined grooves or openings, discrete jacket elements exhibit improved damage tolerance because local defects or cracks are confined within individual components, thereby reducing the risk of catastrophic failure of the entire jacket structure. Third, discrete jackets offer simplified fabrication and assembly processes. Individual jacket elements can be manufactured and assembled separately before being attached to the pressure-bearing cylinder, avoiding the complex interference fitting or prestressing procedures often required to ensure structural continuity in conventional integral jacket designs.

However, the introduction of discrete jacket structures also brings significant challenges to the mechanical analysis of pressure vessels. Conventional analytical solutions for multilayer cylindrical vessels are generally established based on continuous axisymmetric assumptions, where the interaction between adjacent layers can be described through explicit equilibrium and compatibility relationships. Such assumptions become inadequate for discontinuous jacket configurations, where the circumferential stiffness distribution and load transfer mechanisms are strongly affected by the discrete arrangement of external supporting elements. Although finite element analysis (FEA) may provide accurate solutions for these complex structures, its computational cost may become significant during iterative design and optimization processes involving multiple structural parameters. Therefore, an efficient analytical framework capable of capturing the mechanical characteristics of multilayer vessels with discrete jackets is highly desirable.

In this study, a variational semi-analytical framework is proposed for the rapid analysis and design optimization of multilayer cylindrical vessels with discrete jackets. The proposed framework is developed based on the energy formulation of elastic structures and provides an efficient approach for evaluating the mechanical responses of complex multilayer configurations. The effectiveness of the proposed method is demonstrated through finite element simulations of representative vessel designs.

2. The design framework of multilayer pressure vessel with discrete jackets

2.1. The Design Principle of a Multilayer WIP Vessel

In this study, a novel multilayer configuration for WIP equipment is considered, consisting of a core vessel reinforced by two layers of discrete jackets. Global prestressing is introduced through a wire-winding process, which has been widely adopted in the construction of ultra-high-pressure and large-scale vessels due to its capability of accurately controlling and uniformly distributing prestress, as well as its relatively simple and controllable manufacturing procedure.

In the proposed configuration, the inner discrete jacket is designed to provide thermal insulation for the core vessel, which serves as the primary pressure-bearing component, by circulating a heating medium through the jacket channels. The segmented middle cylinder contributes to the overall structural stiffness of the vessel while reducing material consumption and manufacturing cost compared with a fully integrated thick-wall structure. However, elevated operating temperatures may significantly accelerate stress relaxation and creep of prestressing wires. In particular, when the temperature exceeds approximately 80 °C, the degradation of wire prestress becomes increasingly significant [4]. Therefore, an additional external discrete jacket is introduced to circulate a cooling medium, thereby maintaining the mechanical performance and long-term reliability of the wire-wound prestressing system. Each discrete jacket element represents a sector of the original annular structure, and multiple elements are uniformly distributed along the circumference to reconstruct the overall jacket layer.

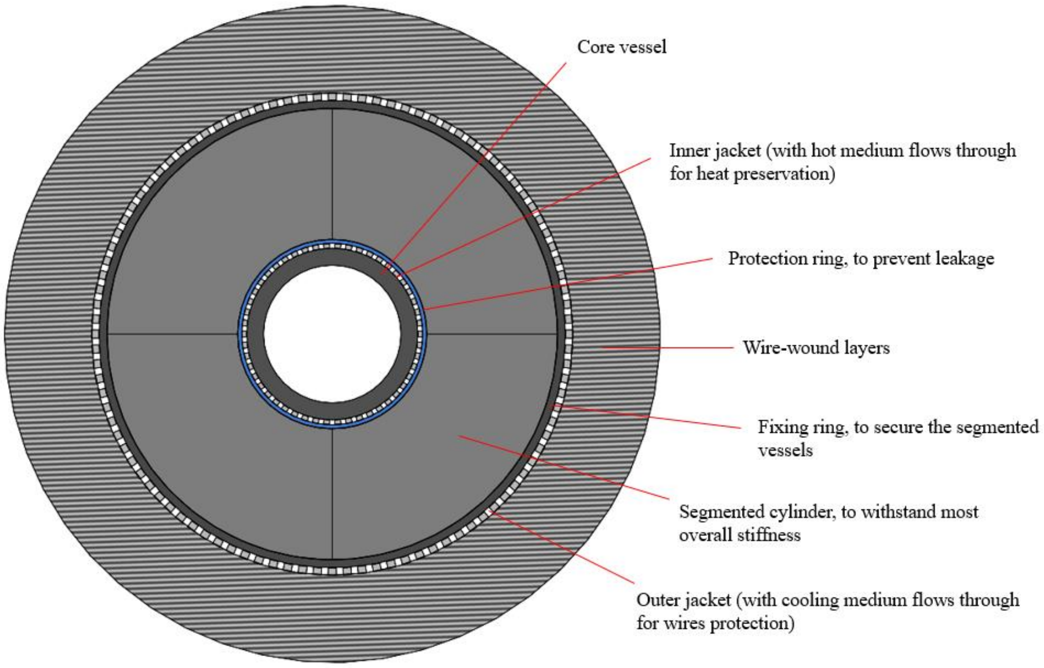

Fig. 1. The schematic of the proposed WIP vessel structure.

2.2. Energy-Based Formulation of Multilayer Cylindrical Vessels under Pressure Loading

Note that, to ensure the fatigue reliability of the vessel under severe cyclic operating conditions, it is desirable to maintain the structural components within the elastic regime throughout the service life, with compressive residual stresses being preferred. The overall mechanical response of the vessel can be obtained through the linear superposition of the effects induced by the internal working pressure and the prestress generated by the winding wires. At each individual winding stage, the contribution of the newly applied wire tension can be equivalently represented as a uniform external pressure acting on the underlying cylindrical structure [5-7]. Therefore, the key challenge is to develop an efficient analytical framework for evaluating the mechanical response of multilayer structures subjected to uniform internal and external pressure loading.

To simplify the analytical formulation, the entire multilayer structure is divided into five equivalent structural regions from the inner to the outer radius. The first region consists of the core vessel. The second region comprises the inner discrete jacket. The third region consists of the rings and segmented vessel components, which are designed to remain primarily under compression and are therefore treated as an equivalent integral region. The fourth region consists of the outer discrete jacket. The fifth region represents the wire-wound layer, whose thickness increases progressively as the winding process proceeds.

Due to the complex local contact behavior and geometric details of individual jacket elements, the mechanical response of a single discrete element is not the primary focus of this study. Instead, the discrete jacket is considered from a macroscopic structural perspective. To ensure an approximately uniform pressure distribution on the surrounding cylindrical layers, the individual jacket elements are assumed to be sufficiently small and uniformly distributed along the circumferential direction. Under this condition, the collective effect of all discrete elements within one jacket layer can be represented by an equivalent continuous layer.

Unlike conventional continuous cylindrical layers, the discrete jacket elements are not interconnected in the circumferential direction and therefore cannot transmit hoop forces between adjacent elements. Based on this characteristic, the discrete jacket layer is modeled as an equivalent thick-walled cylindrical structure with degraded circumferential stiffness, where the hoop stress contribution is neglected. Meanwhile, the interaction between the discrete jacket and neighboring continuous cylindrical layers is represented by a uniformly distributed radial pressure. Consequently, all continuous cylindrical components in the multilayer structure are assumed to satisfy the classical Lamé solution under axisymmetric internal and external pressure loading.

The simplified analytical model and corresponding notations are shown in Fig. 2.

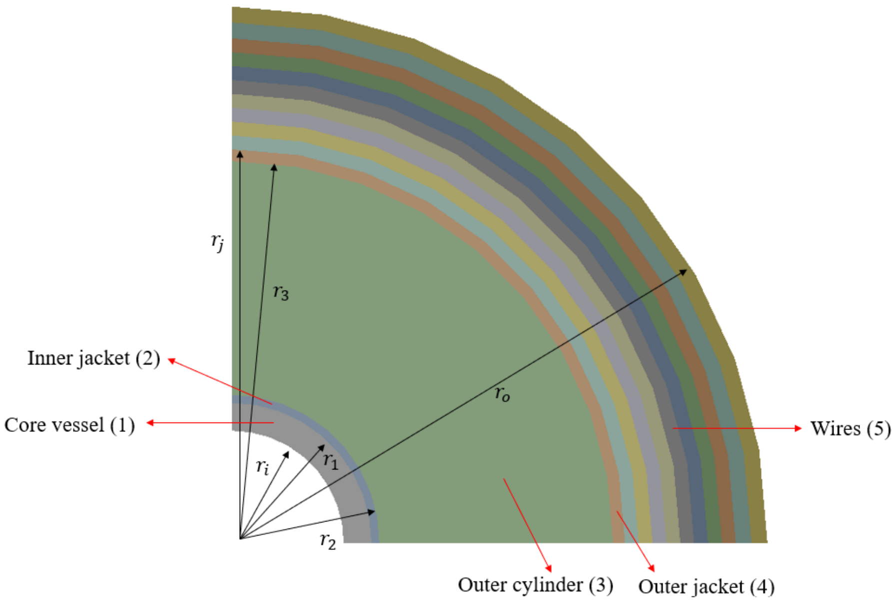

Fig. 2. The simplified analytical model.

Based on the aforementioned assumptions, the mechanical response of the multilayer structure subjected to internal and external pressure loading can be evaluated through the proposed variational framework. For the jacket regions, since circumferential stresses cannot be transmitted between adjacent elements, the equilibrium equation can be expressed as:

$$\frac{d\sigma_r}{dr} + \frac{\sigma_r}{r} = 0 \tag{1}$$

And the corresponding general solution will be:

$$\sigma_r = -\frac{C}{r} \tag{2}$$

Where C is undetermined constant.

For an arbitrary layer within the multilayer structure, the strain energy density u can be expressed as:

$$u = \frac{{\sigma_\theta}^2 + {\sigma_r}^2 - 2v\sigma_\theta\sigma_r}{2E} 2\pi r dr \tag{3}$$

Therefore, the potential energy functional U_n of each region is given by:

$$U_n = \int_{r_{min}}^{r_{max}} \frac{{\sigma_\theta}^2 + {\sigma_r}^2 - 2v\sigma_\theta\sigma_r}{2E} 2\pi r dr \tag{4}$$

Assuming the P_i represents the internal pressure, and P_o represents the external pressure. For the core vessel (region 1), at the interval $[r_i, r_1]$, the boundary condition is: $P_i = P_i, P_o = \frac{C_1}{r_1}$. It can be obtained:

$$A_1 = \frac{{r_i}^2 P_i - {r_1}^2 P_o}{{r_1}^2 - {r_i}^2} = \frac{{r_i}^2 P_i - r_1 C_1}{{r_1}^2 - {r_i}^2} \tag{5}$$

$$B_1 = \frac{{r_i}^2 {r_1}^2 (P_i - P_o)}{{r_1}^2 - {r_i}^2} = \frac{{r_i}^2 r_1 (r_1 P_i - C_1)}{{r_1}^2 - {r_i}^2} \tag{6}$$

Let $a_{10} = \frac{{r_i}^2}{{r_1}^2 - {r_i}^2}$, $a_{11} = -\frac{r_1}{{r_1}^2 - {r_i}^2}$, $b_{10} = \frac{{r_i}^2 {r_1}^2}{{r_1}^2 - {r_i}^2}$, $b_{11} = -\frac{{r_i}^2 r_1}{{r_1}^2 - {r_i}^2}$, then:

$$A_1 = a_{10} P_i + a_{11} C_1 \tag{7}$$

$$B_1 = b_{10} P_i + b_{11} C_1 \tag{8}$$

According to the Lamé solution, the stress distribution of the core vessel will be:

$$\sigma_r^{(1)} = A_1 - \frac{B_1}{r^2} = a_{10} P_i + a_{11} C_1 - \frac{b_{10} P_i + b_{11} C_1}{r^2} = \left(a_{10} - \frac{b_{10}}{r^2}\right) P_i + \left(a_{11} - \frac{b_{11}}{r^2}\right) C_1 \tag{9}$$

$$\sigma_\theta^{(1)} = A_1 + \frac{B_1}{r^2} = a_{10} P_i + a_{11} C_1 + \frac{b_{10} P_i + b_{11} C_1}{r^2} = \left(a_{10} + \frac{b_{10}}{r^2}\right) P_i + \left(a_{11} + \frac{b_{11}}{r^2}\right) C_1 \tag{10}$$

Substituting the Lamé solution into the strain energy density expression, it can be found that the resulting formulation consists of three types of terms, i.e., $\alpha(r) P_i C_1$, $\beta(r) P_i^2$, and $\gamma(r) C_1^2$, where $\alpha(r)$, $\beta(r)$, and $\gamma(r)$are functions solely dependent on the radial coordinate r. Integration of the strain energy over the inner cylinder only modifies the coefficients associated with the radial coordinate, without changing the fundamental form of these terms.

For the inner jacket (region 2), at interval $[r_2, r_3]$, $P_i = \frac{C_1}{r_2}, P_o = \frac{C_2}{r_3}$, thus the stress distributions are:

$$\sigma_r^{(2)} = -\frac{C_1}{r} \tag{11}$$

$$\sigma_\theta^{(2)} = 0 \tag{12}$$

Therefore, its strain energy expression only contains the C_1^2 term.

For the outer cylinder (region 3), at interval $[r_2, r_3]$, $P_i = \frac{C_1}{r_2}, P_o = \frac{C_2}{r_3}$, then:

$$A_2 = \frac{{r_2}^2 P_i - {r_3}^2 P_o}{{r_3}^2 - {r_2}^2} = \frac{r_2 C_1 - r_3 C_2}{{r_3}^2 - {r_2}^2} \tag{13}$$

$$B_2 = \frac{{r_2}^2 {r_3}^2 (P_i - P_o)}{{r_3}^2 - {r_2}^2} = \frac{r_2 {r_3}^2 C_1 - {r_2}^2 r_3 C_2}{{r_3}^2 - {r_2}^2} \tag{14}$$

Let $a_{20} = \frac{r_2}{{r_3}^2 - {r_2}^2}, a_{21} = \frac{-r_3}{{r_3}^2 - {r_2}^2}, b_{20} = \frac{r_2 {r_3}^2}{{r_3}^2 - {r_2}^2}, b_{21} = \frac{-{r_2}^2 r_3}{{r_3}^2 - {r_2}^2}$, it can be obtained:

$$A_2 = a_{20} C_1 + a_{21} C_2 \tag{15}$$

$$B_2 = b_{20} C_1 + b_{21} C_2 \tag{16}$$

Hence the stress distributions of the outer cylinder are:

$$\sigma_r^{(3)} = A_2 - \frac{B_2}{r^2} = a_{20} C_1 + a_{21} C_2 - \frac{b_{20} C_1 + b_{21} C_2}{r^2} = \left(a_{20} - \frac{b_{20}}{r^2}\right) C_1 + \left(a_{21} - \frac{b_{21}}{r^2}\right) C_2 \tag{17}$$

$$\sigma_\theta^{(3)} = A_2 + \frac{B_2}{r^2} = a_{20} C_1 + a_{21} C_2 + \frac{b_{20} C_1 + b_{21} C_2}{r^2} = \left(a_{20} + \frac{b_{20}}{r^2}\right) C_1 + \left(a_{21} + \frac{b_{21}}{r^2}\right) C_2 \tag{18}$$

Substituting into the strain energy formulation, it can be observed that the resulting expression only contains the terms C_1^2, C_2^2, and C_1C_2.

For the outer jacket (region 4), at interval $[r_3, r_j]$, its stress distributions are:

$$\sigma_r^{(4)} = -\frac{C_2}{r} \tag{19}$$

$$\sigma_\theta^{(4)} = 0 \tag{20}$$

Then its strain energy expression only contains the term ${C_2}^2$.

For the wire-wound layer (region 5), the Lamé solution is applied within the region $[r_j, r_o]$, where the equivalent internal pressure is defined as $P_i = C_2/r_j$ and the external pressure is P_o. The mathematical formulation follows the same form as that of the core vessel. Therefore, the corresponding strain energy expression consists of the terms P_oC_2, P_o^2, and C_2^2.

By summing the energy contributions from all individual layers, the total potential energy of the multilayer structure under internal and external pressure loading can be expressed as:

$$U = \sum_{n=1}^{N} U_n \tag{21}$$

For the proposed structure, $N = 5$. Then U can be expressed in the following form:

$$U = \frac{1}{2}K_{11}{C_1}^2 + K_{12}C_1C_2 + \frac{1}{2}K_{22}{C_2}^2 - f_1C_1 - f_2C_2 + U_0 \tag{22}$$

Which is:

$$U = \frac{1}{2}\begin{bmatrix} C_1 & C_2 \end{bmatrix}\begin{bmatrix} K_{11} & K_{12} \\ K_{12} & K_{22} \end{bmatrix}\begin{bmatrix} C_1 \\ C_2 \end{bmatrix} - \begin{bmatrix} f_1 & f_2 \end{bmatrix}\begin{bmatrix} C_1 \\ C_2 \end{bmatrix} + U_0 \tag{23}$$

Or equivalently:

$$U = \frac{1}{2}C^TKC - f^TC + U_0 \tag{24}$$

Here, K is defined as the equivalent stiffness matrix and f is defined as the equivalent external load vector. According to the principle of minimum potential energy, the equilibrium condition is obtained by setting the partial derivative of the total potential energy functional with respect to C to zero:

$$\frac{\partial U}{\partial C} = 0 \rightarrow KC = f \rightarrow C = K^{-1}f \tag{25}$$

It can be observed that the total potential energy U is a strictly quadratic function of the coefficient vector C. For a fixed structural configuration, K remains a constant matrix and is identical to the Hessian matrix of U, i.e., $K = H = \nabla^2 U$.

Thus, the stiffness matrix K is:

$$K = \nabla^2 U \rightarrow K_{ij} = \frac{\partial^2 U}{\partial C_i \partial C_j} \tag{26}$$

And the equivalent load vector is:

$$f = -\nabla U|_{C=0} \rightarrow f_i = -\frac{\partial U}{\partial C_i}|_{C=0} \tag{27}$$

2.3. Semi-Analytical Identification of Structural Stiffness and Load Operators

Since the analytical expression of U is highly complicated, a semi-analytical approach is adopted to extract the stiffness matrix K and the equivalent external load vector f. For a general smooth function, the Taylor expansion at an arbitrary point C_0 can be expressed as:

$$U(C_0 + \Delta C) = U(C_0) + \nabla U(C_0)^T \Delta C + \frac{1}{2}\Delta C^T \nabla^2 U(C_0)\Delta C + R_3 \tag{28}$$

Where R_3 represents the third- and higher-order remainder terms. Since U is a strictly quadratic function, the higher-order terms vanish, i.e., $R_3 = 0$. Therefore, the following expression:

$$U(C_0 + \Delta C) = U(C_0) + \nabla U(C_0)^T \Delta C + \frac{1}{2}\Delta C^T \nabla^2 U(C_0)\Delta C \tag{29}$$

is strictly valid for any choice of the expansion point C_0.

The central difference operators are employed to extract the first- and second-order Taylor coefficients from the sampled function values. For a general function, this extraction process introduces truncation errors associated with the remainder term R_3. However, for a strictly quadratic function, R_3 vanishes, and therefore the central difference operators provide exact identification of the first- and second-order coefficients without truncation errors.

By considering the Taylor expansion at $C = 0$, the stiffness matrix K and the equivalent external load vector f can be obtained as follows:

$$\begin{cases} f_i = -\dfrac{U(he_i) - U(-he_i)}{2h} \\ K_{ii} = \dfrac{U(he_i) - 2U(0) + U(-he_i)}{h^2} \\ K_{ij} = \dfrac{U(he_i + he_j) - U(he_i - he_j) - U(-he_i + he_j) + U(-he_i - he_j)}{4h^2} \end{cases} \tag{30}$$

The energy terms $U(he_i)$, $U(-he_i)$, and other required energy values can be obtained through numerical integration, without requiring an explicit analytical expression of the total potential energy functional.

The stress response function for the multilayer structure under internal and external pressure loading is formulated based on the proposed energy-based variational framework as:

$$\begin{cases} \sigma_\theta^U(r) = \mathcal{L}_\theta^U(P_i, P_o, r_i, r_o; r) \\ \sigma_r^U(r) = \mathcal{L}_r^U(P_i, P_o, r_i, r_o; r) \end{cases} \tag{31}$$

Meanwhile, the stress response function of the multilayer structure treated as an equivalent single thick-walled cylinder (which will be discussed in the subsequent comparisons) subjected to internal and external pressure loading is defined as:

$$\begin{cases} \sigma_\theta^{Lame}(r) = \mathcal{L}_\theta^{Lame}(P_i, P_o, r_i, r_o; r) \\ \sigma_r^{Lame}(r) = \mathcal{L}_r^{Lame}(P_i, P_o, r_i, r_o; r) \end{cases} \tag{32}$$

Here, L_θ^U and L_r^U denote the stress evaluation operators derived from the energy-based formulation, while L_θ^{Lame} and L_r^{Lame} represent the stress evaluation operators based on the equivalent single-cylinder Lamé solution. The feasibility of the proposed energy-based approximation is validated using FEA. Two representative models are considered for verification: an idealized model corresponding to the theoretical limiting configuration, and a realistic model incorporating the discrete jacket structure. For each model, two loading conditions are investigated: (i) $P_i = 660$ MPa, representing the case with internal pressure only; and (ii) $P_o = 300$ MPa, representing an equivalent loading condition during an instantaneous wire-winding stage.

The theoretical predictions from the proposed framework are compared with FEM results obtained from two different models, as shown in Fig. 3. The first model follows the idealized assumption adopted in the analytical formulation, where the jacket regions are represented as equivalent cylindrical layers with zero hoop stress. The second model directly models the actual discrete jacket elements to evaluate the applicability of the proposed approximation under realistic structural conditions.

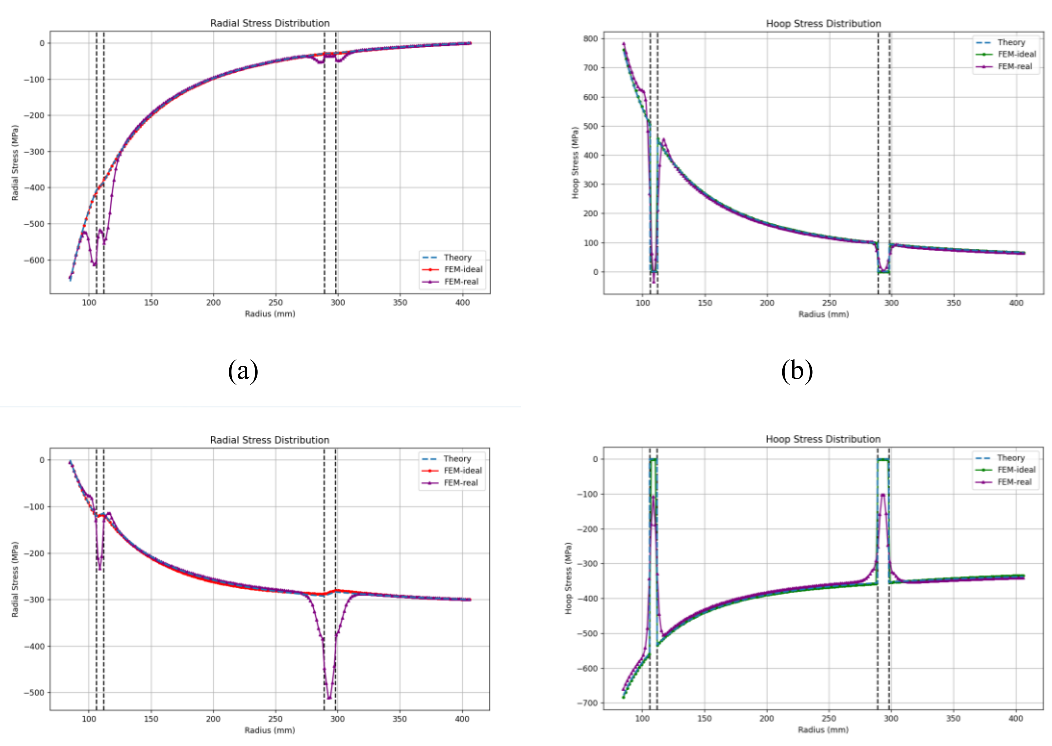

(a) (b)

(c) (d)

Fig. 3. The comparison of theoretical prediction with FEM results, (a) radial stress under internal pressure; (b) hoop stress under internal pressure; (c) radial stress under external pressure; (d) hoop stress under external pressure.

It can be seen that the results from the idealized model agree well with the theoretical predictions. For the realistic discrete model, certain stress fluctuations appear within the jacket regions, which are attributed to the difference between the equivalent representation adopted in the idealized formulation and the local stress concentrations induced by the discrete geometry and boundary conditions. This confirms that the proposed energy-based variational framework is sufficient for capturing the global mechanical response of the multilayer structure.

It should be noted that the proposed energy-based framework is not restricted to the specific structure considered herein. For general multilayer jacketed structures, the total energy functional remains a quadratic form with respect to the unknown interface parameters. Therefore, Eq. (24) provides a generalized formulation, where different configurations only influence the dimension of C.

2.4. Modeling of Layer-Wise Prestress Evolution during Wire Winding

The initial dimensions of the wire-wound vessel are determined by treating the entire multilayer structure as an equivalent integral cylinder. Based on this assumption, the corresponding winding stress distribution is denoted as $\sigma_0(r)$. For a total number of N winding layers, the continuous stress distribution $\sigma_0(r)$ is discretized into stepwise winding stresses $S_w(k)$, where $1 \le k \le N$.

However, since the discrete jacket regions cannot transfer stresses in the circumferential direction, directly applying $S_w(k)$ to the actual multilayer structure would result in an overestimation of the prestress level. Therefore, to ensure that the prestress evolution remains controllable and consistent with the original design objective during the winding process, the stepwise winding stress $S_w(k)$ needs to be appropriately modified.

Let r_w denote the instantaneous winding radius, which can be expressed for the k-th winding layer as:

$$r_w^{(k)} = r_j + (k-1)t \tag{33}$$

The corresponding equivalent external pressure generated by the winding layer is given by:

$$P_w^{(k)} = \frac{S_w(k)t}{r_w^{(k)}} \tag{34}$$

The modified stepwise winding stress after compensation is denoted as $S'_w(k)$. For the equivalent integral cylinder model, the increment of hoop stress at the inner surface of the core vessel caused by each winding layer can be expressed as:

$$\Delta\sigma_{\theta,k}^{Lame}(r_i) = \mathcal{L}_\theta^{Lame}\left(0, P_w^{(k)}, r_i, r_w^{(k)}; r = r_i\right) \tag{35}$$

For the multilayer structure, the increment of inner-wall hoop stress of the core vessel caused by each winding layer is given by:

$$\Delta\sigma_{\theta,k}^{U}(r_i) = \mathcal{L}_\theta^{U}\left(0, P_w^{(k)}, r_i, r_w^{(k)}; r = r_i\right) \tag{36}$$

It should be noted that, to avoid numerical singularity in the evaluation of $L_\theta^U(0, P_w^{(k)}, r_i, r_w^{(k)})$ during the first winding step, a small non-zero thickness is assigned to the wire-wound layer when calculating U_5.

By assuming a unit winding stress for each layer, i.e., $S_w(k) = 1$, the corresponding compensation coefficient can be obtained as:

$$\phi(k) = \frac{\Delta\sigma_{\theta,k}^{U}(r_i)}{\Delta\sigma_{\theta,k}^{Lame}(r_i)} \tag{37}$$

Thus, the modified stepwise winding stress $S'_w(k)$ can be determined:

$$S'_w(k) = \frac{S_w(k)}{\phi(k)} \tag{38}$$

By applying the compensated stepwise winding stress $S'_w(k)$, the stress distribution under the prestress condition (when the wire-winding is accomplished) is subsequently evaluated. The calculation method is as follows:

$$\begin{cases} \sigma_{g\theta}(r) = \sum_{k=1}^{N}\left(\mathcal{L}_\theta^U\left(0, P_w^{(k)}, r_i, r_w^{(k)}; r\right) H\left(r_w^{(k)} - r\right) + S_w(k) H\left(r - r_w^{(k)}\right) H\left(r_w^{(k)} + t - r\right)\right) \\ \sigma_{gr}(r) = \sum_{k=1}^{N}\left(\mathcal{L}_r^U\left(0, P_w^{(k)}, r_i, r_w^{(k)}; r\right) H\left(r_w^{(k)} - r\right)\right) \end{cases} \tag{39}$$

Here, $H(r_w^{(k)} - r)$, $H(r - r_w^{(k)})$, and $H(r_w^{(k)} + t - r)$ represent the corresponding Heaviside step functions, where $r \in [r_i, r_o]$. These functions are introduced to describe the activation of the k-th winding layer during the sequential winding process.

When considering the working condition (when internal design pressure is applied), the stress distributions can be determined as follows:

$$\begin{cases}\sigma_\theta(r) = \sigma_{g\theta}(r) + \mathcal{L}_\theta^U(P_i, 0, r_i, r_o; r) \\ \sigma_r(r) = \sigma_{gr}(r) + \mathcal{L}_r^U(P_i, 0, r_i, r_o; r)\end{cases} \tag{40}$$

3. FEM Validation of the Proposed Framework for a Full-Scale Wire-Wound Multilayer Structure

3.1. Structural Design of the Wire-wound Multilayer Vessel

The initial design of the wire-wound vessel is based on constant von Mises stress winding method [8], which ensures that all the wires sustain constant equivalent stresses in working condition.

The determination of the wire-winding interface r_j is as follows:

$$\begin{cases} P_i \dfrac{{r_j}^2 + {r_i}^2}{{r_j}^2 - r_i^2} + \dfrac{2r_j^2}{{r_j}^2 - r_i^2}\sigma_{r_j} = \dfrac{1-\eta}{\eta}\left|\sigma_{gti}\right| \\ \sigma_r(r) = \dfrac{\sigma_2}{1.0313}\left(\ln\dfrac{r}{r_o} - 0.4121\left(\ln\dfrac{r}{r_o}\right)^2 - 0.2907\left(\ln\dfrac{r}{r_o}\right)^3\right) \\ \sigma_t = \dfrac{\sigma_r + \sqrt{4{\sigma_2}^2 - 3{\sigma_r}^2}}{2} \end{cases} \tag{41}$$

Where σ_{gti} is the prestress at the inner-wall surface of the cylinder, η represents the prestress coefficient (typically >1). σ_2 denotes the design stress of the wires, which is determined according to material specifications.

The theoretical winding stress curve is deduced as follows:

$$\sigma_0(r) = \sigma_{gt} + \left|\sigma_{gr}\right|\frac{r^2 + {r_i}^2}{r^2 - {r_i}^2} \tag{42}$$

Where σ_{gt}, σ_{gr} are hoop and radial stresses of the wires in prestress condition, which can be determined based on the principle of superposition [9-11].

The thickness of the core vessel is designed to prevent buckling under the prestress condition, while the thickness of the jacket layers is determined according to the required flow rate of the heating/cooling medium.

3.2. Determination of Stepwise Winding Stresses

The complete wire-winding process is subsequently simulated. Since the accurate introduction of the prestress field relies on the assumption of a continuous winding interface [12], this assumption is no longer applicable at the discrete jacket boundaries. To ensure numerical convergence and accuracy, the jacket regions modeled in Fig. 2 are represented by an idealized limiting configuration with a regularization treatment, in which the circumferential and radial stiffnesses are assigned with an approximate ratio of at least 1:100, respectively.

In addition, the number of stepwise winding layers is simplified into several groups. Since the stepwise winding scheme is essentially a low-order piecewise approximation of a continuous winding stress function, the continuous distribution function should first be established. Therefore, $\phi(k)$ is reformulated in terms of the continuous radial coordinate as $\phi(r)$.

A set of basis functions is introduced as follows:

$$\phi_{fit}(r) = \frac{a + \frac{b}{r^2}}{1 + \frac{c}{r^2}} \tag{43}$$

The least-squares fitting results are presented in Fig. 4:

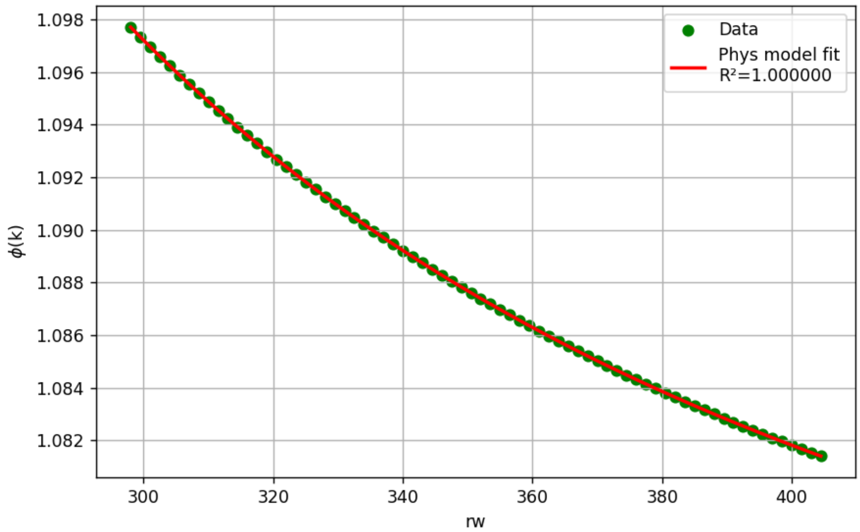

Fig. 4. The fitted continuous curve of the compensation coefficient.

The obtained coefficients are: $a = 1.06417153$, $b = -7.68387126 \times 10^3$, $c = -9.71324314 \times 10^3$ .The coefficient of determination is $R^2 = 1$, indicating an excellent agreement between the fitted function and the discrete data points. The corresponding continuous compensated winding stress distribution can therefore be expressed as:

$$\sigma_0'(r) = \frac{\sigma_0(r)}{\phi_{fit}(r)} \tag{44}$$

Based on the low-order piecewise approximation of the continuous winding stress function, the compensated stepwise winding stresses $S_w'(k)$ can be obtained as follows (simplified to 10 groups):

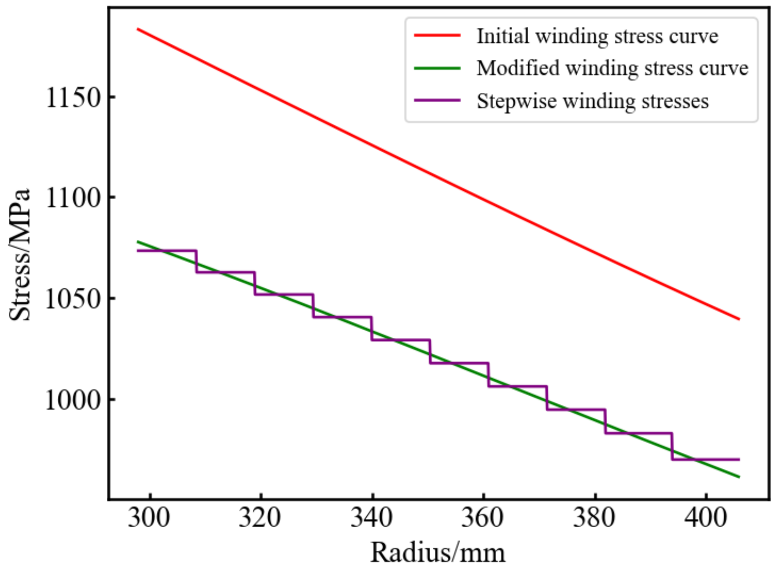

Fig. 5. The initial continuous winding stress curve, the compensated stress curve and the corresponding discrete winding stresses.

The prestress in wire-wound vessels is commonly introduced into the wires using the equivalent thermal strain method [12]. However, for the multilayer configuration considered in this study, the FEA involves coupled thermal–mechanical loading conditions, where artificial thermal strains may conflict with the actual thermal loads. Therefore, an equivalent initial stress method is adopted to introduce the wire-induced prestress.

Based on the principle of displacement continuity at instantaneous winding interfaces, the equivalent initial strain of each wire group can be deduced as follows, and the APDL command is used to introduce the initial stress field.

$$\varepsilon = \frac{S_w'(k)}{E}\left(\frac{{r_{k+1}}^2 + {r_k}^2}{{r_{k+1}}^2 - r_k^2} + \frac{{r_k}^2 + r_i^2}{{r_k}^2 - r_i^2}\right)\frac{{r_k}^2 - {r_i}^2}{2{r_k}^2}\ln\frac{{r_{k+1}}^2 - {r_i}^2}{{r_k}^2 - {r_i}^2} \tag{45}$$

The sequential wire-winding process is simulated by activating the winding layers step by step using the element birth and death technique [8]. The FEM results are compared with the analytical predictions, as shown below.

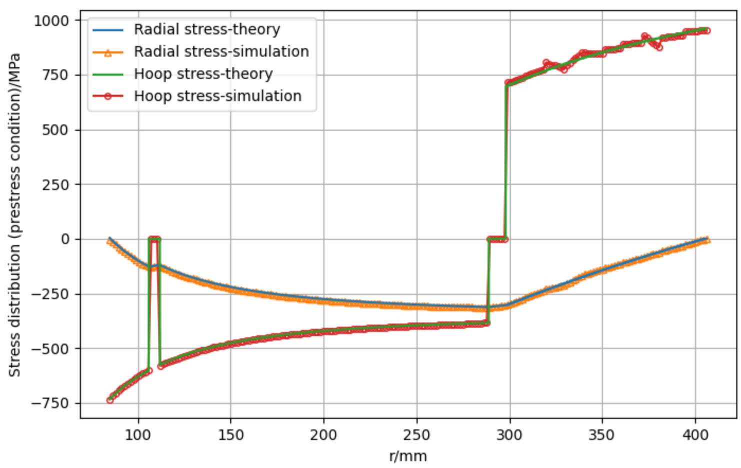

(a)

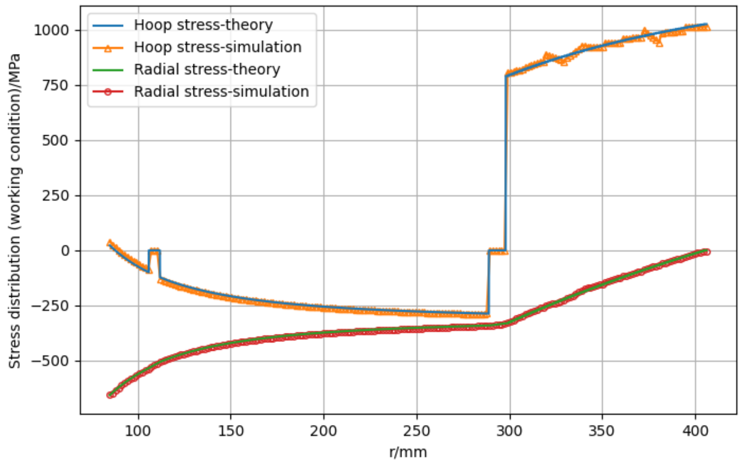

(b)

Fig. 6. The comparison of energy-based theoretical predictions and FEM for full-scale wire-wound multilayer structure, (a) under prestress condition, (b) under working condition.

It can be seen that the FEM results show good agreement with the predictions obtained from the proposed energy-based framework, demonstrating that the proposed semi-analytical approach can effectively predict the stress distribution of wire-wound multilayer structures with discrete jackets. It should be noted that, in the FEM model, the jacket regions are represented as equivalent thick-walled cylindrical layers with regularized hoop stiffness approaching zero, rather than explicitly modelling the actual discrete jacket elements. This treatment is adopted because an accurate introduction of the equivalent wire-induced prestress remains challenging for a structure with discrete components and discontinuous interfaces. Therefore, the present FEM model provides a consistent verification of the proposed theoretical assumptions and the global mechanical response of the multilayer structure.

3.3. Evaluation of the Wire-Wound Multilayer Vessel under Coupled Thermal–Mechanical Loads

The proposed APDL-based initial stress method combined with the element birth and death technique is employed to introduce the prestress field into the model shown in Fig. 2. After all winding groups are fully activated, the design internal pressure of $P_i = 660$ MPa and the design temperature of $T_i = 150$℃ and $T_j = 50$℃ are simultaneously applied. The equivalent stress distribution of the vessel under the resulting steady-state thermo-mechanical condition is then obtained as follows.

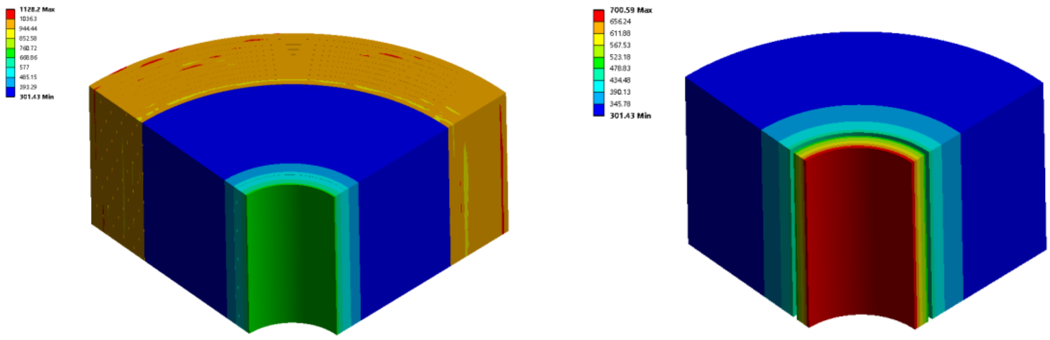

(a) (b)

Fig. 7. The FEM results under coupled thermal-mechanical loads, (a) the equivalent stress contour of the overall wire-wound multilayer structure, (b) the equivalent stress contour of the core vessel and the outer cylinder(s).

It can be seen that, under the steady-state thermal insulation and pressure-holding condition, the equivalent stress in the wires remains well below the yield strength of the wire material (1600–1800 MPa). Meanwhile, the equivalent stress of the core vessel is also below its yield strength, with a maximum value of approximately 831 MPa. The outer cylinder(s), which provide the primary structural stiffness, exhibit an equivalent stress level also remaining below their yield strength of approximately 500MPa. Therefore, the proposed multilayer wire-wound vessel configuration satisfies the required structural strength under the designed thermo-mechanical operating condition.

4. Conclusions

In this study, a variational energy-based semi-analytical framework was proposed for the efficient analysis of multilayer wire-wound cylindrical vessels containing discrete jacket structures. By considering the characteristics of discrete jacket elements, where circumferential stress transfer between adjacent elements is negligible, the jacket regions were represented as equivalent cylindrical layers with zero hoop stress. Based on this assumption, the stress response of multilayer structures subjected to internal and external pressures was derived through a variational formulation. The proposed framework provides a direct and efficient approach for evaluating the mechanical response of complex multilayer configurations without requiring detailed modelling of individual jacket elements.

A semi-analytical procedure was further developed to extract the stiffness matrix and equivalent load vector from the energy functional. Since the total energy function of the considered system is a strict quadratic form, the required coefficients can be accurately obtained through numerical differentiation without truncation errors. The proposed method was subsequently extended to simulate the sequential wire-winding process by introducing compensated stepwise winding stresses, ensuring that the prestress evolution of the core vessel remains consistent with the original design target.

Furthermore, the proposed framework is not limited to the specific multilayer configuration investigated in this study. Owing to the quadratic form of the total energy functional for general multilayer jacketed structures within the linear elastic framework, the developed formulation can be extended to various multilayer configurations with different numbers and arrangements of jacket layers. The variation among different structures only affects the dimension of the interface parameter vector, while the fundamental solution procedure remains unchanged.

The proposed framework was verified through FE simulations. The theoretical predictions showed good agreement with the FEM results for both radial and hoop stress distributions, demonstrating the effectiveness of the proposed approach. Furthermore, the application to a full-scale wire-wound multilayer vessel under coupled thermal–mechanical loading conditions confirmed that the proposed structure can satisfy the required strength requirements under the designed operating conditions.

It should be noted that the present FEM verification was performed using an equivalent jacket model with regularized hoop stiffness rather than explicitly modelling the actual discrete jacket elements. Future work will therefore focus on developing a more advanced FEM methodology capable of simulating full-scale vessels with realistic discrete jacket elements while maintaining accurate prestress introduction. In addition, a prototype WIP vessel for solid-state batteries manufacturing will be fabricated to experimentally validate the proposed semi-analytical framework. The layer-by-layer deformation of the core vessel during the winding process will be monitored and compared with the theoretical predictions, providing direct verification of the predicted prestress evolution.

References

[1] M.B. Dixit, C. Beamer, M.R. Amin, J. Shipley, R. Eklund, N. Muralidharan, L. Lindqvist, A. Fritz, R. Essehli, M. Balasubramanian, I. Belharouak, The role of isostatic pressing in large-scale production of solid-state batteries, ACS Energy Lett. 7 (11) (2022) 3936–3946.

[2] M. Campéon, P. Porion, A. Pradel, S. Laruelle, Virtues of cold isostatic pressing for preparation of all-solid-state batteries with poly(ethylene oxide), ChemSusChem 17 (2024) e202301054.

[3] K. Hayashi, T. Mori, K. Fukuda, H. Ito, Y. Manabe, Application of warm isostatic pressing to densification of all-solid-state composite cathode electrodes in all-solid-state lithium-ion batteries, J. Jpn. Soc. Powder Powder Metall. 72 (Suppl.) (2025) S1167–S1173.

[4] F. Lin, Z.L. Lin, L. Zhang, Y.N. Yan, R.J. Zhang, Application of prestressed wire-winding technology in forging/extrusion presses, China Metal Forming Equip. Manuf. Technol 45 (1) (2010) 37–42.

[5] ASME, Boiler and Pressure Vessel Code: Section VIII, Division 3: Alternative Rules for Construction of High Pressure Vessels, American Society of Mechanical Engineers, New York, 2025.

[6] M. Sedighi, A.H. Jabbari, Investigation of residual stresses in thick-walled vessels with combination of autofrettage and wire-winding, Int. J. Pressure Vessels Piping 111 (2013) 295–301.

[7] M. Elfar, R. Sedaghati, O.R. Abdelsalam, Analytical formulation to predict residual stresses in thick-walled cylinders subjected to hoop winding, shrink-fit, and conventional and reverse autofrettages, J. Pressure Vessel Technol. 146 (2) (2024) 021501.

[8] Y. Huang, Z. Li, Z. Lv, W. Qi, C. Duan, B. Wang, A design approach for wire-wound ultra-high pressure vessels in isostatic pressing systems based on constant von Mises stress criterion, Int. J. Pressure Vessels Piping 218 (2025) 105730.

[9] Y.N. Yan, Design and calculation of prestressed wire wound cylinders, J. Tsinghua Univ. (Sci. Technol.) 4 (1978) 106–119.

[10] J. Gronbaek, T. Wanheim, Optimum design of ribbon and wire wound cylinders for metal forming dies, J. Eng. Ind. 99 (3) (1977) 733–737.

[11] L.Y. Maksimov, Design of cylinder to withstand high internal pressure, Russ. Eng. J. 44 (5)

(1964).
[12] J.M. Alegre, P. Bravo, M. Preciado, Simulation procedure of high pressure vessels using the wire winding technique, Eng. Fail. Anal. 17 (1) (2010) 61–69.